

Article

Extracting Hypernuclear Properties from the $(e, e'K^+)$ Cross Section

Omar Benhar

INFN and Department of Physics, Sapienza University, 00185 Rome, Italy; omar.benhar@roma1.infn.it

Abstract: Experimental studies of hypernuclear dynamics, besides being essential for the understanding of strong interactions in the strange sector, have important astrophysical implications. The observation of neutron stars with masses exceeding two solar masses poses a serious challenge to the models of hyperon dynamics in dense nuclear matter, many of which predict a maximum mass incompatible with the data. In this paper, it is argued that valuable new insight can be gained from the forthcoming extension of the experimental studies of kaon electro production from nuclei to include the $^{208}\text{Pb}(e, e'K^+)^{208}_{\Lambda}\text{Tl}$ process. A comprehensive framework for the description of kaon electro production, based on factorization of the nuclear cross section and the formalism of the nuclear many-body theory, is outlined. This approach highlights the connection between the kaon production and proton knockout reactions, which will allow us to exploit the available $^{208}\text{Pb}(e, e'p)^{207}\text{Tl}$ data to achieve a largely model-independent analysis of the measured cross section.

Keywords: kaon electro production; hyperon dynamics; strange hadronic matter



Citation: Benhar, O. Extracting Hypernuclear Properties from the $(e, e'K^+)$ Cross Section. *Particles* **2021**, *4*, 194–204. <https://doi.org/10.3390/particles4020018>

Academic Editor: Armen Sedrakian

Received: 22 March 2021

Accepted: 6 May 2021

Published: 11 May 2021

Publisher's Note: MDPI stays neutral with regard to jurisdictional claims in published maps and institutional affiliations.



Copyright: © 2021 by the author. Licensee MDPI, Basel, Switzerland. This article is an open access article distributed under the terms and conditions of the Creative Commons Attribution (CC BY) license (<https://creativecommons.org/licenses/by/4.0/>).

1. Introduction

Experimental studies of the $(e, e'K^+)$ reaction on nuclei have long been recognized as a valuable source of information on hypernuclear spectroscopy. The extensive program of measurements performed or approved at Jefferson Lab [1,2]—encompassing a variety of nuclear targets ranging from ^6Li to ^{40}Ca and ^{48}Ca —has the potential to shed new light on the dynamics of strong interactions in the strange sector, addressing outstanding issues such as the isospin-dependence of hyperon-nucleon interactions and the role of three-body forces involving nucleons and hyperons. In addition, because the appearance of hyperons is expected to become energetically favored in dense nuclear matter, these measurements have important implications for neutron star physics.

The recent observation of two-solar-mass neutron stars [3,4]—the existence of which is ruled out by many models predicting the presence of hyperons in the neutron star core [5]—suggests that the present understanding of nuclear interactions involving hyperons is far from being complete. In the literature, the issue of reconciling the calculated properties of hyperon matter with the existence of massive stars is referred to as the *hyperon puzzle* [6].

Owing to the severe difficulties involved in the determination of the potential describing hyperon–nucleon (YN) interactions from scattering data, the study of hypernuclear spectroscopy provides an effective alternative approach, capable of yielding much needed additional information.

In this context, the $(e, e'K^+)$ process offers clear advantages. The high resolution achievable by γ -ray spectroscopy can only be exploited to study energy levels below nucleon emission threshold, while (K^-, π^-) and (π^+, K^+) reactions mainly provide information on non-spin-flip interactions. Moreover, compared to hadron induced reactions, kaon electro production allows a better energy resolution, which may in turn result in a more accurate identification of the hyperon binding energies [1]. However, the results of several decades of study of the $(e, e'p)$ reaction show that, to achieve this goal, the analysis

of the measured cross sections must be based on a theoretical model taking into account the full complexity of electron-nucleus interactions [7]. Addressing this issue will be critical to the recently approved extension of the Jefferson Lab program to the case of a heavy target with large neutron excess, the nucleus ^{208}Pb . This experiment will allow us to study hyperon dynamics in an environment providing the best available proxy of the neutron star interior. A short account of the proposal to measure the $^{208}\text{Pb}(e, e'K^+)_{\Lambda}^{208}\text{Tl}$ cross section in Jefferson Lab Hall A can be found in Ref. [8].

This work is meant to lay down the foundations of a comprehensive theoretical framework for the description of the $(e, e'K^+)$ cross section within the formalism of nuclear many-body theory, which has been extensively and successfully employed to study the proton knockout reaction [7]. In addition, it is shown that, owing to the connection between the $(e, e'p)$ and $(e, e'K^+)$ processes which naturally emerges in the context of the proposed analysis, the missing energy spectra measured in $(e, e'p)$ experiments provide the baseline needed for a largely model-independent determination of the hyperon binding energies.

The body of this paper is structured as follows. In Section 2, the treatment of kaon electro-production from nuclei in the kinematical regime in which factorization of the nuclear cross section is expected to be applicable is derived, and the relation to the proton knockout process is highlighted. The main conceptual issues associated with the description of the elementary electron–proton vertex and the nuclear amplitudes comprising the structure of the $^{208}\text{Pb}(e, e'K^+)_{\Lambda}^{208}\text{Tl}$ cross section are discussed in Section 3. Finally, the summary and an outlook to future developments can be found in Section 4.

2. The $A(e, E'K^+)_{\Lambda}A$ Cross Section

Let us consider the kaon electro-production process:

$$e(k) + A(p_A) \rightarrow e'(k') + K^+(p_K) + {}_{\Lambda}A(p_R), \tag{1}$$

in which an electron scatters off a nucleus of mass number A , and the hadronic final state

$$|F\rangle = |K^+ {}_{\Lambda}A\rangle, \tag{2}$$

includes a K^+ meson and the recoiling hypernucleus, resulting from the replacement of a proton with a Λ in the target nucleus. The incoming and scattered electrons have four-momenta, $k \equiv (E, \mathbf{k})$ and $k' \equiv (E', \mathbf{k}')$, respectively, while the corresponding quantities associated with the kaon and the recoiling hypernucleus are denoted by $p_K \equiv (E_K, \mathbf{p}_K)$ and $p_R \equiv (E_R, \mathbf{p}_R)$. Finally, in the lab reference frame—in which the lepton kinematical variables are measured— $p_A \equiv (M_A, 0)$.

The differential cross section of reaction (1) can be written in the form

$$d\sigma_A \propto L_{\mu\nu} W^{\mu\nu} \delta^{(4)}(p_A + q - p_F), \tag{3}$$

with $\lambda, \mu = 1, 2, 3$, where $q = k - k'$ and $p_F = p_K + p_R$ are the four-momentum transfer and the total four-momentum carried by the hadronic final state, respectively. The tensor $L_{\mu\nu}$, fully specified by the electron kinematical variables, can be written in the form [9]

$$L = \begin{pmatrix} \eta_+ & 0 & -\sqrt{\epsilon_L \eta_+} \\ 0 & \eta_- & 0 \\ -\sqrt{\epsilon_L \eta_+} & 0 & \epsilon_L \end{pmatrix}, \tag{4}$$

with $\eta_{\pm} = (1 \pm \epsilon)/2$ and

$$\epsilon = \left(1 + 2 \frac{|\mathbf{q}|^2}{Q^2} \tan^2 \frac{\theta_e}{2}\right)^{-1}, \tag{5}$$

where θ_e is the electron scattering angle, $q \equiv (\omega, \mathbf{q})$, $Q^2 = -q^2$, and $\epsilon_L = \epsilon Q^2/\omega^2$.

All the information on hadronic, nuclear and hypernuclear dynamics is contained in the nuclear response tensor, defined as

$$W^{\mu\nu} = \langle 0 | J_A^{\mu\dagger}(q) | F \rangle \langle F | J_A^\nu(q) | 0 \rangle, \tag{6}$$

where $|0\rangle$ denotes the target ground state, and the final state $|F\rangle$ is given by Equation (2).

Equation (6) shows that the theoretical calculation of the cross section requires a consistent description of the nuclear and hypernuclear wave functions, as well as of the nuclear current operator appearing in the transition matrix element, J_A^μ . This problem, which in general involves prohibitive difficulties, is greatly simplified in the kinematical region in which the impulse approximation can be exploited.

2.1. Impulse Approximation and Factorization

Figure 1 provides a diagrammatic representation of the $(e, e' K^+)$ process based on the factorization *ansatz*.

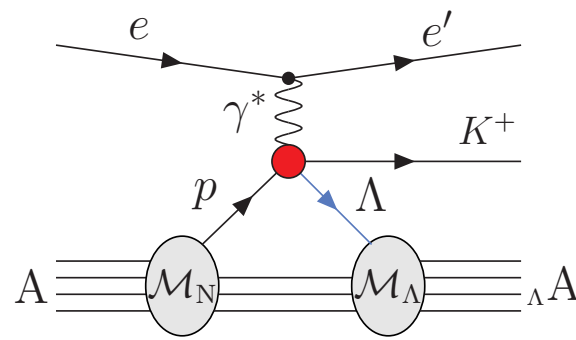


Figure 1. Schematic representation of the scattering amplitude associated with the process of Equation (1) in the impulse approximation regime.

The formalism exploiting factorization of the nuclear cross section is expected to be applicable in the impulse approximation regime, corresponding to momentum transfer such that the wavelength of the virtual photon, $\lambda \sim 1/|\mathbf{q}|$, is short compared to the average distance between nucleons in the target nucleus, $d_{NN} \sim 1.5$ fm.

Under these conditions, which can be easily met at Jefferson Lab—hereafter JLab—the beam particles primarily interact with individual protons, the remaining $A - 1$ nucleons acting as spectators. As a consequence, the nuclear current operator reduces to the sum of one-body operators describing the electron-proton interaction

$$J_A^\mu(q) = \sum_{i=1}^A j_i^\mu(q), \tag{7}$$

and the hadronic final state takes the product form

$$|F\rangle = |K^+\rangle \otimes |\Lambda A\rangle, \tag{8}$$

with the outgoing K^+ being described by a plane wave, or by a distorted wave obtained from a kaon-nucleus optical potential [1].

From the above equations, it follows that the nuclear transition amplitude

$$\mathcal{M}^\mu = \langle K^+ \Lambda A | J_A^\mu(q) | 0 \rangle, \tag{9}$$

can be written in factorized form through insertion of the completeness relations

$$\int \frac{d^3 p}{(2\pi)^3} |\mathbf{p}\rangle \langle \mathbf{p}| = \int \frac{d^3 p_\Lambda}{(2\pi)^3} |\mathbf{p}_\Lambda\rangle \langle \mathbf{p}_\Lambda| = \mathbf{1}, \tag{10}$$

where the integrations over the momenta carried by the proton and the Λ also include spin summations, and

$$\sum_n |(A-1)_n\rangle\langle(A-1)_n| = \mathbf{1}, \quad (11)$$

the sum being extended to all eigenstates of the $(A-1)$ -nucleon spectator system.

The resulting expression turns out to be

$$\mathcal{M}^\mu = \sum_{i=1}^A \sum_n \int \frac{d^3p}{(2\pi)^3} \frac{d^3p_\Lambda}{(2\pi)^3} \mathcal{M}_{\Lambda A \rightarrow (A-1)_{n+\Lambda}}^* \langle \mathbf{p}_K \mathbf{k}_\Lambda | j_i^\mu | \mathbf{p} \rangle \mathcal{M}_{A \rightarrow (A-1)_{n+p}}, \quad (12)$$

where the current matrix element describes the elementary electromagnetic process $\gamma^* + p \rightarrow K^+ + \Lambda$.

Note that, compared to the case of nucleon knock out discussed in, e.g., Ref. [10], the transition amplitude describing kaon production within the factorization scheme, Equation (12), exhibits a more complex structure, involving two different amplitudes.

The nuclear and hypernuclear amplitudes in the right-hand side of Equation (12), labeled \mathcal{M}_N and \mathcal{M}_Λ in Figure 1, are given by

$$\mathcal{M}_{A \rightarrow (A-1)_{n+p}} = \{ \langle \mathbf{p} | \otimes \langle (A-1)_n | \} | 0 \rangle, \quad (13)$$

and

$$\mathcal{M}_{\Lambda A \rightarrow (A-1)_{n+\Lambda}} = \{ \langle \mathbf{p}_\Lambda | \otimes \langle (A-1)_n | \} | \Lambda A \rangle. \quad (14)$$

In the above equations, the states $|(A-1)_n\rangle$ and $|\Lambda A\rangle$ describe the $(A-1)$ -nucleon spectator system, appearing as an intermediate state, and the final-state Λ -hypernucleus, respectively.

The amplitudes of Equation (13) determine the Green's function $G(\mathbf{k}, E)$ —embodying all information on single-particle dynamics in the target nucleus—and the associated spectral function, defined as

$$P(\mathbf{k}, E) = \frac{1}{\pi} \text{Im} G(\mathbf{k}, E) \quad (15)$$

$$= \sum_n |\mathcal{M}_{A \rightarrow (A-1)_{n+p}}|^2 \delta(E + M_A - m - E_n),$$

where m is the nucleon mass and E_n denotes the energy of the $(A-1)$ -nucleon system in the state n . The spectral function describes the *joint* probability to remove a nucleon of momentum \mathbf{k} from the nuclear ground state, leaving the residual system with excitation energy $E > 0$.

Note that within the mean-field approximation, underlying the nuclear shell model, Equation (15) reduces to the simple form

$$P(\mathbf{k}, E) = \sum_{\alpha \in \{F\}} |\varphi_\alpha(\mathbf{k})|^2 \delta(E - |\epsilon_\alpha|), \quad (16)$$

where $\alpha \equiv \{nj\ell\}$ is the set of quantum numbers specifying single-nucleon orbits. The sum is extended to all states belonging to the Fermi sea, the momentum-space wave functions and energies of which are denoted $\varphi_\alpha(\mathbf{k})$ and ϵ_α , respectively, with $\epsilon_\alpha < 0$.

Equation (16) shows that within the independent particle model, the spectral function reduces to a set of δ -function peaks, representing the energy spectrum of single-nucleon states. Dynamical effects beyond the mean field shift the position of the peaks, that also acquire a finite width. In addition, the occurrence of virtual scattering processes—bringing about the excitation of nucleon pairs to continuum states above the Fermi surface—leads to the appearance of a sizable smooth contribution to the Green's function, accounting for $\sim 20\%$ of the total strength. As a consequence, the normalization of a shell model state φ_α , referred to as spectroscopic factor, is reduced from unity to a value $Z_\alpha < 1$.

The nuclear spectral functions have been extensively studied measuring the cross section of the $(e, e'p)$ reaction, in which the scattered electron and the knocked out nucleon are detected in coincidence. The results of these experiments, carried out using a variety of nuclear targets, have unambiguously identified the states predicted by the shell model, at the same time highlighting the limitations of the mean-field approximation and the effects of nucleon–nucleon correlations [7,11,12].

In analogy with Equations (13) and (15), the amplitudes of Equation (14) comprise the spectral function

$$P_{\Lambda}(\mathbf{k}_{\Lambda}, E_{\Lambda}) = \sum_n |\mathcal{M}_{\Lambda A \rightarrow (A-1)_n + \Lambda}|^2 \delta(E_{\Lambda} + M_{\Lambda A} - M_{\Lambda} - E_n), \quad (17)$$

describing the joint probability to remove a Λ from the hypernucleus ${}_{\Lambda}A$, leaving the residual system with energy E_{Λ} . Here, M_{Λ} and $M_{\Lambda A}$ denote the mass of the Λ and the hypernucleus, respectively.

The observed $(e, e'K^+)$ cross section, plotted as a function of the missing energy

$$E_{\text{miss}}^{\Lambda} = \omega - E_{K^+}, \quad (18)$$

exhibits a collection of peaks, providing the sought-after information on the energy spectrum of the Λ in the final state hypernucleus. In principle, the right-hand side of Equation (18) should also include a term accounting for the kinetic energy of the recoiling hypernucleus. However, for heavy targets, this contribution turns out to be negligibly small, and will be omitted. Note that both the electron energy loss, ω , and the energy of the outgoing kaon, E_{K^+} , are *measured* kinematical quantities.

2.2. Kinematics

The expression of $E_{\text{miss}}^{\Lambda}$, Equation (18), can be conveniently rewritten considering that the δ -function of Equation (3) implies the condition

$$\omega + M_A = E_{K^+} + E_{\Lambda A}. \quad (19)$$

Combining the above relation with the requirement of conservation of energy at the nuclear and hypernuclear vertices, dictating

$$M_A = E_p + E_n, \quad E_{\Lambda} + E_n = E_{\Lambda A}, \quad (20)$$

we find

$$\omega + E_p = E_{K^+} + E_{\Lambda}. \quad (21)$$

Finally, substitution into Equation (18) yields

$$E_{\text{miss}}^{\Lambda} = E_{\Lambda} - E_p. \quad (22)$$

The above equation, while providing a relation between the *measured* missing energy and the binding energy of the Λ in the final state hypernucleus, defined as $B_{\Lambda} = -E_{\Lambda}$, *does not* allow for a model-independent identification of E_{Λ} . The position of a peak observed in the missing energy spectrum turns out to be determined by the difference between the energies needed to remove a Λ from the final state hypernucleus, E_{Λ} , or a proton from the target nucleus, E_p , leaving the residual $(A - 1)$ -nucleon system in the *same* bound state, specified by the quantum numbers collectively denoted n .

The proton removal energies, however, can be *independently* obtained from the missing energy *measured* by proton knockout experiments—in which the scattered electron and the ejected proton are detected in coincidence—defined as

$$E_{\text{miss}}^p = \omega - E_{p'} = -E_p. \quad (23)$$

where E_p is the energy of the outgoing proton. Note that, consistently with Equation (18), the kinetic energy of the recoiling nucleus has been omitted in the right-hand side of the above equation.

From Equations (22) and (23), it follows that the Λ binding energy can be determined in a fully model-independent fashion from

$$B_\Lambda = -E_\Lambda = -(E_{\text{miss}}^\Lambda - E_{\text{miss}}^p), \tag{24}$$

combining the information provided by the missing energy spectra measured in $(e, e'K^+)$ and $(e, e'p)$ experiments.

3. The $^{208}\text{Pb}(e, E'K^+)^{208}_\Lambda\text{Tl}$ Cross Section

In view of astrophysical applications, the recently approved measurement of the $^{208}\text{Pb}(e, e'K^+)^{208}_\Lambda\text{Tl}$ cross section at JLab [8] will be of utmost importance. In this section, I will review the basic elements of the theoretical description of kaon electro production within the factorization scheme laid down in Section 2.

3.1. The $E + P \rightarrow E' + K^+ + \Lambda$ Process

The description of the elementary $e + p \rightarrow e' + K^+ + \Lambda$ process involving an isolated proton at rest has been obtained from the isobar model [13,14], in which the hadron current is derived from an effective Lagrangian comprising baryon and meson fields. Different implementations of this model are characterized by the intermediate states appearing in processes featuring the excitation of resonances [15–17]. The resulting expressions—involving a set of free parameters determined by fitting the available experimental data—have been used to obtain nuclear cross sections within the approach based on the nuclear shell model and the frozen-nucleon approximation [1,15].

In principle, the calculation of the nuclear cross section within the scheme outlined in Section 2.1 should be performed by taking into account that the elementary process involves a bound, moving nucleon, with four-momentum $p \equiv (E_p, \mathbf{p})$ and energy

$$E_p = M_A - E_n = m - E, \tag{25}$$

as prescribed by Equation (15). However, the generalization to off-shell kinematics of phenomenological approaches constrained by free proton data, such as the isobar model of Refs. [15–17], entails non-trivial conceptual difficulties.

A simple procedure to overcome this problem is based on the observation that in the scattering process on a bound nucleon, a fraction $\delta\omega$ of the energy transfer goes to the spectator system. The amount of energy given to the struck proton, the expression of which naturally emerges from the impulse approximation formalism, turns out to be [10]

$$\tilde{\omega} = \omega - \delta\omega = \omega + m - E - \sqrt{m^2 + \mathbf{p}^2}. \tag{26}$$

Note that from the above equations, it follows that

$$E_p + \omega = \sqrt{m^2 + \mathbf{p}^2} + \tilde{\omega}, \tag{27}$$

implying in turn

$$(p + q)^2 = (\tilde{p} + \tilde{q})^2 = W^2, \tag{28}$$

with $\tilde{q} \equiv (\tilde{\omega}, \mathbf{q})$ and $\tilde{p} \equiv (\sqrt{m^2 + \mathbf{p}^2}, \mathbf{p})$.

The above equations show that the replacement $q \rightarrow \tilde{q}$ allows us to establish a correspondence between electron scattering on an *off-shell* moving proton, leading to the appearance of a final state of invariant mass W , and the corresponding process involving a proton *in free space*. As a consequence, within this scheme the use of an elementary cross section designed to explain hydrogen data is fully consistent.

It has to be mentioned that, although quite reasonable on physics grounds, the use of \tilde{q} in the hadron current leads to a violation of current conservation. This issue is inherent in the impulse approximation scheme, which does not allow us to simultaneously conserve energy and current in correlated systems. A very popular and effective workaround for this problem, widely employed in the analysis of $(e, e'p)$ data, was first proposed by de Forest in the 1980s [18].

In view of the fact that the extension of the work of Refs. [16,17] to the case of a moving proton does not involve severe conceptual difficulties, the consistent application of the formalism developed for proton knock-out processes to the case of kaon electro production appears to be feasible. In this context, it should also be pointed out that the factorization scheme discussed in Section 2 allows for a fully relativistic treatment of the electron-proton vertex, which is definitely required in the kinematical region accessible at JLab [10].

3.2. Nuclear and Hypernuclear Dynamics

Valuable information needed to obtain Λ removal energies from the cross section of the $^{208}\text{Pb}(e, e'K^+)^{208}_{\Lambda}\text{Tl}$ process, using the procedure described in Section 2.2, has been gained by the high-resolution studies of the $^{208}\text{Pb}(e, e'p)^{207}\text{Tl}$ reaction performed at NIKHEF-K in the late 1980s and 1990s [19–22]. The available missing energy spectra—measured with a resolution of better than 100 KeV and extending up to ~ 30 MeV—provide both position and width of the peaks corresponding to bound states of the recoiling ^{207}Tl nucleus.

It is very important to realize that a meaningful interpretation of NIKHEF-K data requires the use of a theoretical framework taking into account effects of nuclear dynamics beyond the mean-field approximation. This issue is clearly illustrated in Figures 2 and 3.

Figure 2 displays the difference between the energies corresponding to the peaks in the measured missing energy spectrum, $\langle E_{\alpha}^p \rangle$, and the predictions of the mean-field model reported in Ref. [23], E_{α}^{MF} . It is apparent that the discrepancy, measured by the quantity

$$\Delta_{\alpha} = |E_{\alpha}^{MF} - \langle E_{\alpha}^p \rangle|, \tag{29}$$

where the index $\alpha \equiv \{nj\ell\}$ specifies the state of the recoiling system, is sizable, and as large as ~ 3 MeV for deeply bound states.

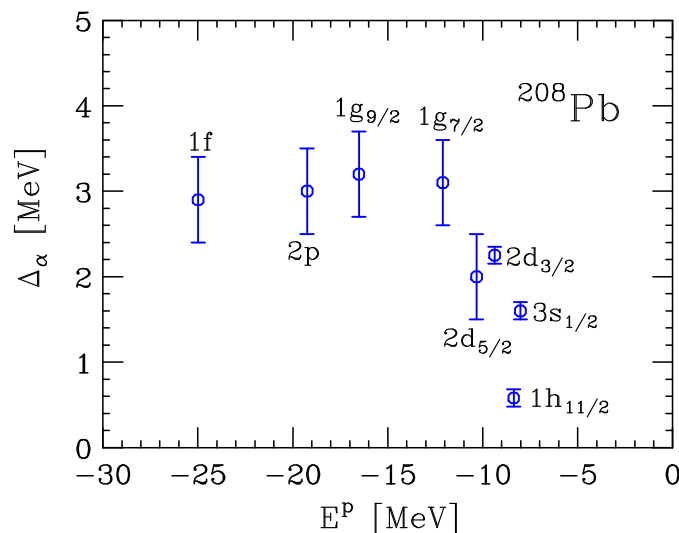


Figure 2. Difference between the energies corresponding to the peaks of the missing energy spectrum of the $^{208}\text{Pb}(e, e'p)^{207}\text{Tl}$ reaction reported in Ref. [19] and the results of the mean-field calculations of Ref. [23], displayed as a function of the proton binding energy $E_p = -E_{\text{miss}}^p$. The states are labeled according to the standard spectroscopic notation.

In Figure 3, the spectroscopic factors extracted from NIKHEF-K data are compared to the results of the theoretical analysis of Ref. [24]. The solid line, exhibiting a remarkable

agreement with the experiment, has been obtained combining theoretical nuclear matter results, displayed by the dashed line, and a phenomenological correction to the imaginary part of the nucleon self-energy, accounting for finite size and shell effects. The energy dependence of the spectroscopic factors of nuclear matter at equilibrium density has been derived from a calculation of the pole contribution to the spectral function of Equation (15), carried out using Correlated Basis Function (CBF) perturbation theory and a microscopic nuclear Hamiltonian including phenomenological two- and three-nucleon potentials [25].

The results of Figure 3 show that the spectroscopic factors of ^{208}Pb , defined as

$$Z_\alpha = \int \frac{d^3k}{(2\pi)^3} |\chi_\alpha(\mathbf{k})|^2, \quad (30)$$

with $\chi_\alpha(\mathbf{k})$ being the Fourier transform of the overlap between the target ground state and the state of the recoiling nucleus, featuring a hole in the shell model orbit α . It appears that, in the case of deeply bound proton states, Z_α is largely determined by short-range correlations, moving strength to the continuum component of the spectral function. As a consequence, they are largely unaffected by surface and shell effect, and can be accurately estimated using the results of nuclear matter calculations. Finite size effects, mainly driven by long-range nuclear dynamics, are more significant in the vicinity of the Fermi surface, where they account for up to $\sim 35\%$ of the deviation from the prediction obtained using the mean field spectral function of Equation (16), represented by the solid horizontal line.

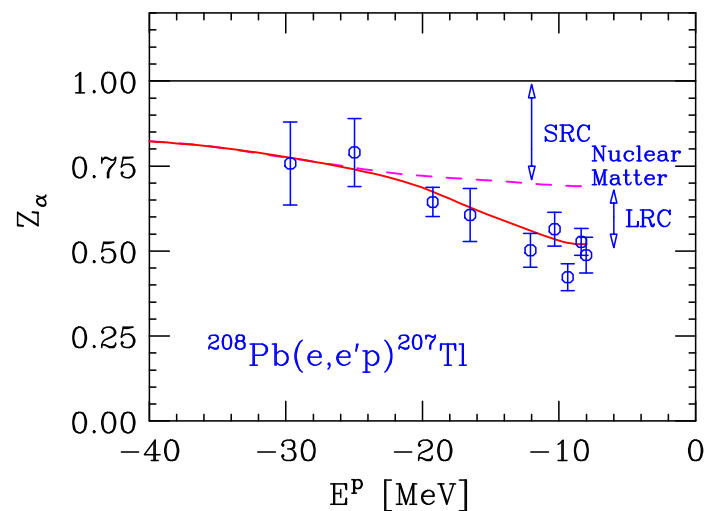


Figure 3. Spectroscopic factors of the shell model states of ^{208}Pb , obtained from the analysis of the $^{208}\text{Pb}(e, e'p)^{207}\text{Tl}$ cross section measured at NIKHEF-K [19]. The dashed line represent the results of theoretical calculations of the spectroscopic factors of nuclear matter, while the solid line has been obtained, including corrections taking into account finite size and shell effects in ^{208}Pb [24]. For comparison, the horizontal line shows the prediction of the spectral function of Equation (16). The deviations arising from short- and long-range correlations are highlighted and labeled SRC and LRC, respectively.

In addition to the nucleon spectral function, the analysis of the $^{208}\text{Pb}(e, e'K^+)^{208}_{\Lambda}\text{Tl}$ cross section requires a consistent description of the Λ spectral function, defined by Equation (17). Following the pioneering nuclear matter study of Ref. [26], microscopic calculations of $P_\Lambda(\mathbf{k}_\Lambda, E_\Lambda)$ in a variety of hypernuclei, ranging from $^5_\Lambda\text{He}$ to $^{208}_\Lambda\text{Pb}$, have been recently carried out by the author of Ref. [27]. In this work, the self-energy of the Λ —simply related to the corresponding Green’s function—was obtained from G -matrix perturbation theory in the Brueckner–Hartree–Fock approximation, using the Jülich [28,29] and Nijmegen [30–32] models of the YN potential.

The generalization of the approach of Ref. [27]—needed to treat $^{208}_{\Lambda}\text{Tl}$ using Hamiltonians including both YN and YNN potentials—does not appear to involve severe difficulties, of either conceptual or technical nature. Therefore, a consistent description of the $^{208}\text{Pb}(e, e'K^+)^{208}_{\Lambda}\text{Tl}$ process within the factorization scheme derived in this work is expected to be achievable within the time frame relevant to the JLab experimental program.

Different computational approaches, mostly based on the Monte Carlo method [33], have been very successful in obtaining ground-state expectation values of Hamiltonians involving nucleons and hyperons, needed to model the equation of state of strange baryon matter, see, e.g., Ref. [6]. However, the present development of these techniques does not allow the calculation of either $(e, e'p)$ or $(e, e'K^+)$ cross sections, most notably in the kinematical regime in which the underlying non-relativistic approximation is no longer applicable. On the other hand, the approach based on factorization, allowing for a fully relativistic treatment of the electron-proton interaction, has proved very effective for the interpretation of the body of available $(e, e'p)$ data.

4. Summary and Outlook

The results discussed in this paper—in which kaon electro production from nuclei is analyzed within the framework of many-body theory using, for the first time, the Green's function formalism—show that valuable new information on hypernuclear dynamics can be obtained from the $^{208}\text{Pb}(e, e'K^+)^{208}_{\Lambda}\text{Tl}$ cross section, the measurement of which in JLab Hall A has been recently approved [8]. In this context, an important role will be played by the availability of accurate missing energy spectra measured by $^{208}\text{Pb}(e, e'p)^{207}\text{Tl}$ experiments, which can be employed to obtain a largely model-independent determination of the Λ binding energies in $^{208}_{\Lambda}\text{Tl}$.

Owing to the extended region of constant density, ^{208}Pb is the best available proxy for uniform nuclear matter. This feature, which also emerges from the results displayed in Figure 3, will be critical to acquire new information on three-body forces, complementary to that obtainable using a calcium target.

The results of accurate many-body calculations of the ground-state energies of finite nuclei [34] and isospin-symmetric nuclear matter [35]—performed with the *same* nuclear Hamiltonian, including the Argonne v_{18} [36] and Urbana IX [37] NN and NNN interaction models, respectively—show that the potential energy per nucleon arising from three-nucleon interactions is a monotonically increasing function of A , whose value changes sign, varying from -0.23 MeV in ^{40}Ca to 2.78 MeV in nuclear matter at equilibrium density. Therefore, constraining three-body forces in the mass region in which their effect changes from attractive to repulsive in the non-strange sector appears to be needed, especially in view of astrophysical applications involving matter at supranuclear densities, in which three-body interactions are known to play a critical role.

The solution of the so-called *hyperon puzzle* is likely to require a great deal of theoretical and experimental work for many years to come. The extension of the JLab kaon electro production program to ^{208}Pb has the potential to provide an important contribution, needed to broaden the present understanding of hypernuclear dynamics in nuclear matter.

Funding: This work was supported by the Italian National Institute for Nuclear Research (INFN) under grant TEONGRAV.

Institutional Review Board Statement: Not applicable.

Informed Consent Statement: Not applicable.

Data Availability Statement: References to all data discussed in the paper are given in the bibliography.

Acknowledgments: The author is deeply indebted to Petr Bydžovský, Franco Garibaldi and Isaac Vidaña for many illuminating discussions on issues related to the subject of this article.

Conflicts of Interest: The author declares no conflict of interest.

References

1. Garibaldi, F.; Acha, A.; Ambrozewicz, P.; Aniol, K.A.; Baturin, P.; Benaoum, H.; Benesch, J.; Bertin, P.Y.; Blomqvist, K.I.; Boeglin, W.U.; et al. High-resolution hypernuclear spectroscopy at Jefferson Lab, Hall A. *Phys. Rev. C* **2019**, *99*, 054309. [[CrossRef](#)]
2. Nakamura, S. Spectroscopy of electro-produced hypernuclei at JLab. *AIP Conf. Proc.* **2019**, *2130*, 020012.
3. Demorest, P.; Pennucci, T.; Ransom, S.; Roberts, M.; Hessels, J. A two-solar-mass neutron star measured using Shapiro delay. *Nature* **2010**, *467*, 1081–1083. [[CrossRef](#)]
4. Antoniadis, J.; Freire, P.C.; Wex, N.; Tauris, T.M.; Lynch, R.S.; van Kerkwijk, M.H.; Kramer, M.; Bassa, C.; Dhillon, V.S.; Driebe, T.; et al. A massive pulsar in a compact relativistic binary. *Science* **2013**, *340*, 6131. [[CrossRef](#)] [[PubMed](#)]
5. Vidaña, I.; Logoteta, D.; Providência, C.; Polls, A.; Bombaci, I. Estimation of the effect of hyperonic three-body forces on the maximum mass of neutron stars. *EPL* **2011**, *94*, 11002. [[CrossRef](#)]
6. Lonardonì, D.; Lovato, A.; Gandolfi, S.; Pederiva, F. Hyperon puzzle: Hints from quantum Monte Carlo calculations. *Phys. Rev. Lett.* **2015**, *114*, 092301. [[CrossRef](#)] [[PubMed](#)]
7. Benhar, O. Exploring nuclear dynamics with $(e, e'p)$ reactions: From LNF to JLab. *Nucl. Phys. News* **2016**, *26*, 15–20. [[CrossRef](#)]
8. Garibaldi, F.; Benhar, O.; Bydžovský, P.; Covrig, S.; Gogami, T.; Markowitz, P.E.C.; Millener, D.J.; Nakamura, S.N.; Reinhold, J.; Tang, L.; et al. Studying Λ interactions in nuclear matter with the $^{208}\text{Pb}(e, e'K^+)^{208}\text{Atl}$ reaction. *AIP Conf. Proc.* **2019**, *2130*, 040003.
9. Amaldi, E.; Fubini, S.; Furlan, G. *Pion Electroproduction*; Springer: Berlin, Germany, 1979.
10. Benhar, O.; Day, D.; Sick, I. Inclusive quasielastic electron-nucleus scattering. *Rev. Mod. Phys.* **2008**, *80*, 189. [[CrossRef](#)]
11. Frullani, S.; Mougey, J. Single-particle properties of nuclei through $(e, e'p)$ reactions. *Adv. Nucl. Phys.* **2016**, *26*, 1.
12. Dieperink, A.E.L.; Huberts, P.K.A. On high resolution $(e, e'p)$ reactions. *Ann. Rev. Nucl. Part. Sci.* **1990**, *40*, 239–284. [[CrossRef](#)]
13. Adam, J., Jr.; Mareš, J.; Richter, O.; Sotona, M.; Frullani, S. Electroproduction of strangeness. *Czech. J. Phys.* **1992**, *42*, 1167–1196. [[CrossRef](#)]
14. David, J.C.; Fayard, C.; Lamot, G.H.; Saghai, B. Electromagnetic production of associated strangeness. *Phys. Rev. C* **1996**, *53*, 2613. [[CrossRef](#)]
15. Sotona, M.; Frullani, S. Electroproduction of strangeness and spectroscopy of light hypernuclei. *Prog. Theor. Phys. Suppl.* **1994**, *117*, 151–175. [[CrossRef](#)]
16. Skoupil, D.; Bydžovský, P. Photoproduction of $K\Lambda$ on the proton. *Phys. Rev. C* **2016**, *93*, 025204. [[CrossRef](#)]
17. Skoupil, D.; Bydžovský, P. Photo-and electroproduction of $K^+ \Lambda$ with a unitarity-restored isobar model. *Phys. Rev. C* **2018**, *97*, 025202. [[CrossRef](#)]
18. de Forest, T., Jr. Off-shell electron-nucleon cross sections: The impulse approximation. *Nucl. Phys. A* **1983**, *392*, 232–248. [[CrossRef](#)]
19. Quint, E.N.M. Limitations of the Mean-Field Description for Nuclei in the Pb-Region, Observed with the $(e, e'p)$ Reaction. Ph.D. Thesis, University of Amsterdam, Amsterdam, The Netherlands, 1988.
20. Quint, E.N.M.; van den Brand, J.F.J.; den Herder, J.W.A.; Jans, E.; Keizer, P.H.M.; Lapikás, L.; van der Steenhoven, G.; de Witt Huberts, P.K.A.; Klein, S.; Grabmayr, P.; et al. Relative $3s$ Spectroscopic Strength in ^{206}Pb and ^{208}Pb Studied with the $(e, e'p)$ Knockout Reaction. *Phys. Rev. Lett.* **1986**, *57*, 186. [[CrossRef](#)]
21. Bobeldijk, I.; Bouwhuis, M.; Irel, D.G.; De Jager, C.W.; Jans, E.; de Jonge, N.; Kasdorp, W.J.; Konijn, J.; Lapikás, L.; van Leeuwe, J.J.; et al. High-Momentum Protons in ^{206}Pb . *Phys. Rev. Lett.* **1994**, *73*, 2684. [[CrossRef](#)] [[PubMed](#)]
22. Bobeldijk, I.; Blok, H.P.; van den Brink, H.B.; Dodge, G.E.; Hesselink, W.H.A.; Jans, E.; Kasdorp, W.J.; Lapikas, L.; van Leeuwe, J.J.; March, C.; et al. Search for nucleon-nucleon correlations in the proton spectral function of ^{208}Pb . *Phys. Lett. B* **1995**, *353*, 32–38. [[CrossRef](#)]
23. Negele, J.W.; Vautherin, D. Density-matrix expansion for an effective nuclear hamiltonian. *Phys. Rev. C* **1972**, *5*, 1472. [[CrossRef](#)]
24. Benhar, O.; Fabrocini, A.; Fantoni, S. Occupation probabilities and hole-state strengths in nuclear matter. *Phys. Rev. C* **1990**, *41*, R24. [[CrossRef](#)]
25. Benhar, O.; Fabrocini, A.; Fantoni, S. The nucleon spectral function in nuclear matter. *Nucl. Phys. A* **1989**, *505*, 267–299. [[CrossRef](#)]
26. Robertson, N.J.; Dickhoff, W.H. Correlation effects on Λ propagation in nuclear matter. *Phys. Rev. C* **2004**, *70*, 044301. [[CrossRef](#)]
27. Vidaña, I. Single-particle spectral function of the Λ hyperon in finite nuclei. *Nucl. Phys. A* **2017**, *958*, 48–70. [[CrossRef](#)]
28. Holzenkamp, B.; Holinde, K.; Speth, J. A meson exchange model for the hyperon-nucleon interaction. *Nucl. Phys. A* **1989**, *500*, 485–528. [[CrossRef](#)]
29. Heidenbauer, J.; Meissner, U.G. Jülich hyperon-nucleon model revisited. *Phys. Rev. C* **2005**, *72*, 044005. [[CrossRef](#)]
30. Maesen, P.M.M.; Rijken, T.A.; de Swart, J.J. Soft-core baryon-baryon one-boson-exchange models. II. Hyperon-nucleon potential. *Phys. Rev. C* **1989**, *40*, 2226. [[CrossRef](#)] [[PubMed](#)]
31. Rijken, T.A.; Stoks, V.J.G.; Yamamoto, Y. Soft-core hyperon-nucleon potentials. *Phys. Rev. C* **1999**, *59*, 21. [[CrossRef](#)]
32. Stoks, V.J.G.; Rijken, T.A. Soft-core baryon-baryon potentials for the complete baryon octet. *Phys. Rev. C* **1999**, *59*, 3009. [[CrossRef](#)]
33. Carlson, J.; Gandolfi, S.; Pederiva, F.; Pieper, S.C.; Schiavilla, R.; Schmidt, K.; Wiringa, R.B. Quantum Monte Carlo methods for nuclear physics. *Rev. Mod. Phys.* **2015**, *87*, 1067. [[CrossRef](#)]
34. Lonardonì, D.; Lovato, A.; Pieper, S.C.; Wiringa, R.B. Variational calculation of the ground state of closed-shell nuclei up to $A = 40$. *Phys. Rev. C* **2017**, *96*, 024326. [[CrossRef](#)]

-
35. Akmal, A.; Pandharipande, V.R.; Ravenhall, D.G. Equation of state of nucleon matter and neutron star structure. *Phys. Rev. C* **1998**, *58*, 1804. [[CrossRef](#)]
 36. Wiringa, R.B.; Stoks, V.G.J.; Schiavilla, R. Accurate nucleon-nucleon potential with charge-independence breaking. *Phys. Rev. C* **1995**, *51*, 38. [[CrossRef](#)]
 37. Pudliner, B.S.; Pandharipande, V.R.; Carlson, J.; Wiringa, R.B. Quantum Monte Carlo calculations of $A \leq 6$ nuclei. *Phys. Rev. Lett.* **1995**, *74*, 4396. [[CrossRef](#)] [[PubMed](#)]